Scheme III

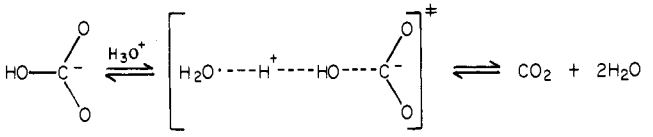

questionable, for the following reason: the rate constant for unimolecular decomposition of H_2CO_3 is 18 s^{-1} (ref 13). This rate constant is related to Scheme II by the equilibrium constant for the interconversion

$$H_2CO_3 \rightleftharpoons H_2O^+-CO_2^-$$

If this equilibrium constant is about 10^{-8}, then the actual rate constant for decomposition of the zwitterion in Scheme II is about 10^9 s^{-1}, which is near the diffusion-controlled limit; if the equilibrium constant is less than this value (as might easily be the case), then the mechanism of Scheme II is impossible because the required rate of decomposition of the zwitterionic intermediate exceeds the diffusion-controlled limit.

The solvent isotope effect on the dehydration of HCO_3^- ($k_{H_3O^+}/k_{D_3O^+} = 0.56$) is similar in magnitude to solvent isotope effects observed in A-1 type cleavages in which the transition state is product-like.[13] However, if the mechanism shown in Scheme II is correct, then carbon isotope effects indicate that the transition state must be reactant-like, and this should give a solvent isotope effect near unity. Thus, it appears that the mechanism shown in Scheme II is not correct.

The alternative to the specific-acid-catalyzed mechanism of Scheme II is a general-acid-catalyzed mechanism, as suggested by Pocker and Bjorquist[13] (Scheme III), in which H_3O^+ serves as a general acid and H^+ transfer is concerted with C–O bond breaking. Again, the carbon isotope effect indicates an early transition state. The solvent isotope effects, small salt also consistent with such a scheme. This mechanism also avoids the diffusion-control problem which occurs with Scheme II. The carbon and solvent isotope effect studies, taken together, appear to favor this mechanism over that shown in Scheme II.

Acknowledgment. This work was supported by NSF Grant PCM-8216597. We are grateful to C. A. Roeske for running the ^{13}C NMR spectra.

Registry No. ^{13}C, 14762-74-4; CO_2, 124-38-9; HCO_3^-, 71-52-3.

Effect of Free Energy on Rates of Electron Transfer between Molecules[1]

John R. Miller,* James V. Beitz, and R. Kurt Huddleston

Contribution from the Chemistry Division, Argonne National Laboratory, Argonne, Illinois 60439. *Received November 21, 1983*

Abstract: Rates of electron-transfer (ET) reactions $D^- + A \rightarrow D + A^-$ between aromatic molecules in a rigid organic solid have been measured from 10^{-7} to 10^2 s following creation of radical anions by pulse radiolysis. By avoiding the problems of diffusion control and complexing between the donor and acceptor which occur in liquids, these data provide the first opportunity to interpret measurements of electron-transfer rates vs. exothermicity with ET theories. Reactions having free energy changes from $-\Delta G° = 0.01$ to 2.75 eV were studied. For each reaction, the ET rate constant $k(r)$ is quantitatively measured as a function of distance using the random distribution of distances between D^-, A pairs. The ET rates are very slow for weakly exothermic reactions, are maximized at an intermediate exothermicity λ, and decrease at high exothermicity. λ is observed to increase gradually with time, due apparently to solvent relaxation around D^- ions suddenly formed in the rigid medium. Because this causes the distance dependence of the rates to vary with exothermicity, quantitative comparison of the data with ET theories is possible only if we assume that the distance dependence of electron exchange interactions does not depend on the acceptor. This assumption, which is consistent with elementary theories of electron exchange interactions, allows the following conclusion to be drawn from the data: (1) The rate vs. energy relation at a given time can be described by standard ET theories which consider reorganization of both low-frequency solvent modes and high-frequency molecular vibrations. (2) An empirical dependence of the solvent reorganization energy (λ_s) on time, obtained from the shift of the peak of the rate vs. $\Delta G°$ curve, gives good account of the shapes of the kinetic decay curves but underestimates the rates for highly exothermic reactions. (3) No information is obtained about the effect of molecular orientation, but the orientation-averaged rates may be extrapolated to shorter distances to estimate a rate of $10^{13.3}$ s^{-1} for optimally exothermic ET between species in contact at 296 K. (4) Because this contact rate is more than 2 orders of magnitude larger than necessary for diffusion control, the rate constants for diffusional ET reactions in fluids are expected to provide little information about dependence of rates on exothermicity. (5) The rates decrease exponentially with distance $k(r) = \nu \exp(-r/a)$ with $a = 0.83$ Å.

1. Introduction

A. Background on Energy vs. Electron-Transfer Rates. Theories of electron-transfer (ET) processes in condensed media[2-21] have consistently predicted a relationship between kinetics and thermodynamics: Rates are expected to be slow for weakly exothermic

(1) Work supported by the U.S. Department of Energy, Division of Chemical Science, under Contract W-31-109-ENG-39.
(2) Marcus, R. A. *J. Chem. Phys.* **1956**, *24*, 966.
(3) Levich, V. O. *Adv. Electrochem. Electrochem. Eng.* **1966**, *4*, 249.
(4) Dogonadze, R. R. In "Reactions of Molecules at Electrodes"; Hush, N. S., Ed.; Wiley-Interscience: New York, 1971.
(5) Grigorov, L. N.; Chernavskii, D. S. *Biophysics (Engl. Transl.)* **1972**, *17*, 202. Blumenfeld, L. A.; Chernavskii, D. S. *J. Theor. Biol.* **1973**, *39*, 1.
(6) Hush, N. S. *Trans. Faraday Soc.* **1961**, *57*, 577.
(7) (a) Kestner, N. R.; Jortner, J.; Logan, J. *J. Phys. Chem.* **1974**, *78*, 2148. (b) Webman, I.; Kestner, N. R. *J. Chem. Phys.* **1982**, *77*, 2387.
(8) Van Duyne, R. P.; Fischer, S. F. *Chem. Phys.* **1974**, *5*, 183.
(9) Fischer, S. F.; Van Duyne, R. P. *Chem. Phys.* **1977**, *26*, 9.
(10) Ulstrup, J.; Jortner, J. J. *Chem. Phys.* **1975**, *63*, 4358.
(11) Newton, M. D. *Int. J. Quantum Chem. Symp.* **1980**, *14*, 363. Brunschwig, B. S.; Logan, J.; Newton, M.; Sutin, N. *J. Am. Chem. Soc.* **1980**, *102*, 5798.
(12) Jortner, J. *J. Chem. Phys.* **1976**, *64*, 4860.
(13) (a) Dogonadze, R. R.; Kuznetsov, A. M.; Vorotyntsev, M. A.; Zakaroya, M. G. J. *Electroanal. Chem.* **1977**, *75*, 315. (b) Dogonadze, R. R.; Kuznetsov, A. M.; Vorotyntsev, M. A. *Z. Phys. Chem. N. F.* **1976**, *100*, 1.
(14) (a) Hopfield, J. J. *Proc. Natl. Acad. Sci. U.S.A.* **1974**, *71*, 3640. (b) Reference 15, p 417. (c) Redi, M.; Hopfield, J. J. *Chem. Phys.* **1980**, *72*, 6651.

0002-7863/84/1506-5057$01.50/0

reactions, to increase to a maximum for moderately exothermic reactions, and then to *decrease* with increasing exothermicity for highly exothermic ET reactions. This expected dependence of rate on energy is due to simultaneous requirements for conservation of energy and nuclear position during electron transfer. The reactants must be converted into products having vibrational (and possibly electronic) excitation equal to the reaction exothermicity, but the nuclear configuration of reactants and products must be the same according to the Franck–Condon principle.

A number of experimental studies of ET reactions in solution have failed to find that ET rates decrease at high exothermicities; instead the rate constants reach the diffusion controlled limit at moderate exothermicities (0.3–0.6 eV) and remain there to the highest exothermicities attainable.[22-34] Isolated instances of slower rates were reported,[34-37] but the preponderance of data[22-34] against these exothermic Franck–Condon restrictions have led to serious doubts that they occur and a suggestion that they should not even have been expected.[32,33]

Measurements of reactions of trapped electrons in a glassy solid[38,39] showed that large exothermicities did decrease ET rates by factors as large as 10^5. We suggested then[38] that such solid-state ET reactions provided the best tests of the true dependence of energy on rate, whereas ET reactions in fluids were seriously complicated by the leveling effect of the diffusion controlled limit and by the probable formation of complexes.

That first study[38,39] of the effect of energy on ET rate in a glassy matrix had some disadvantages: (1) The electron donor was the trapped electron (e_t^-), which is an unusual chemical species. It is possible to imagine that the slow rates of highly exothermic reactions are peculiar to e_t^-. (2) Because the redox potential of e_t^- can only be approximately estimated, only relative reaction exothermicities were precisely known. (3) About two-thirds of the highly exothermic reactions had sufficient exothermicity to produce products (radical anions of the acceptors) in electronically excited states. Thus, the plot of $-\Delta G$ vs. rate therefore appeared as a "shotgun pattern" of scattered points in the highly exothermic region. (4) The weakly exothermic region was not characterized because redox potentials were not known for the appropriate acceptors. (5) The reaction medium is a low-temperature glass, which may be imagined to be untypical.

This work remedies the first four of the above difficulties. The reactions are of the type

$$D^- + A \rightarrow D + A^- \quad (1)$$

where the electron donors (D^-) are radical anions of aromatic hydrocarbons (usually biphenyl in this study), in which the excess electron occupies a π^* orbital. The electron acceptors (A) are organic, usually aromatic, molecules. The reaction exothermicities are accurately known from reduction potentials (polarography, voltametry, potentiometry) and in some cases measurements of intermolecular electron-transfer equilibria. Because the biphenyl anion (Bip^-) is a less powerful reducing agent than e_t^-, reaction channels producing electronically excited products are unimportant in most cases. As we shall argue below, because of limitations of measurements in liquids, this is the first study in any condensed medium which meaningfully measures the effect of exothermicity on ET rates over the full range. An additional method[40,41] which substitutes various quinones into reaction centers of photosynthetic bacteria is beginning to yield important results in Dutton's laboratory.[40]

Recently, in collaboration with Closs, we have measured ET rate constants at a fixed distance in fluid solution at room temperature by fixing the donor and acceptor to a rigid spacer.[42] With this technique, both the decrease of rate at large $-\Delta G°$ and astonishing effects of solvent polarity are observed.[42b] Reorganization parameters obtained from the rate vs. $\Delta G°$ curve are in very good agreement with those to be reported herein.

B. Electron-Transfer Theory and Solid-State Electron Transfer. Pulse radiolysis experiments in solids have made possible measurements of ET rate as a function of distance[38,39,43-54] between the reactants as well as measurements as a function of reaction exothermicity.[38,39] This section briefly reviews ET theory.

The rate constant for electron transfer from an electron donor to an electron acceptor at distance (center to center) r is given by[2-21]

$$k = (2\pi/\hbar)|V(r)|^2 \text{ FCWD} \quad (2)$$

The rate expression has two parts: the electron exchange matrix element, $V(r)$, and the Franck–Condon weighted density of states, FCWD. $V(r)$ measures the weak interaction between the tails of the wave functions for the electron on the donor and on the acceptor and falls exponentially with distance beyond the contact distance R_o.

(15) Chance, B.; De Vault, D.; Frauenfelder, H.; Marcus, R.; Schrieffer, J.; Sutin, N. "Tunneling in Biological Systems"; Academic Press: New York, 1979.
(16) Ulstrup, J. "Charge Transfer Processes in Condensed Media"; Springer-Verlag: Berlin, 1979.
(17) Kuznetsov, A. M.; Ulstrup, J. *J. Chem. Phys.* **1981**, *75*, 2047. Kuznetsov, A. M.; Søndergard, N. C.; Ulstrup, J. *Chem. Phys.* **1978**, *29*, 383.
(18) Schmitt, P. P. In "Electrochemistry"; The Chemical Society: London, 1977; (a) Vol. 5, p 26; (b) Vol. 6, p 128.
(19) Kakitani, T.; Kakatani, H. *Biochem. Biophys. Acta* **1981**, *635*, 498.
(20) De Vault, D. *Q. Rev. Biophys.* **1980**, *13*, 387.
(21) Duke, C. B. *Phys. Rev. B: Solid State* **1981**, *23*, 2111.
(22) Rehm, D.; Weller, A. *Isr. J. Chem.* **1970**, *8*, 259.
(23) Bock, C. R.; Meyer, T. J.; Whitten, D. G. *J. Am. Chem. Soc.* **1975**, *97*, 2909.
(24) Nagle, J. K.; Dresick, W. J.; Meyer, T. J. *J. Am. Chem. Soc.* **1979**, *101*, 3993.
(25) Vogelmann, E.; Schreiner, S.; Rauscher, W.; Kramer, H. *Z. Phys. Chem. N. F.* **1976**, *101*, 321.
(26) Ramonahov, L. V.; Kiryakhin, Y. I.; Bagddasar'yan, K. S. *Dokl. Phys. Chem. (Engl. Transl.)* **1976**, *230*, 961.
(27) Scheerer, R.; Gratzel, M. *J. Am. Chem. Soc.* **1977**, *99*, 865.
(28) Eriksen, J.; Forte, C. S. *J. Phys. Chem.* **1978**, *82*, 2659.
(29) Breymann, V.; Dreeskamp, H.; Koch, E.; Zander, M. *Chem. Phys. Lett.* **1978**, *59*, 68.
(30) Ballardini, R.; Varani, G.; Indelliu, M. T.; Scandola, F.; Balzani, V. *J. Am. Chem. Soc.* **1978**, *100*, 7219.
(31) Balzani, V.; Bolletta, F.; Gandolfi, M. T.; Maestri, M. *Top. Curr. Chem.* **1978**, *75*, 1.
(32) Scandola, F.; Balzani, V. *J. Am. Chem. Soc.* **1979**, *101*, 6140.
(33) Balzani, V.; Scandola, F.; Orlandi, G.; Sabbantini, N.; Indelli, M. T. *J. Am. Chem. Soc.* **1981**, *103*, 3370.
(34) Creutz, C.; Sutin, N. *J. Am. Chem. Soc.* **1977**, *99*, 241.
(35) Frank, A.; Grätzel, M.; Henglein, A.; Janata, E. *Ber. Bunsenges. Phys. Chem.* **1976**, *80*, 547. Henglein, A. *Can. J. Chem.* **1977**, *55*, 2112.
(36) Jonah, C. D.; Matheson, M. S.; Meisel, D. *J. Am. Chem. Soc.* **1978**, *100*, 449.
(37) Wallace, W. L.; Bard, A. J. *J. Phys. Chem.* **1979**, *83*, 1350.
(38) Beitz, J. V.; Miller, J. R. *J. Chem. Phys.* **1979**, *71*, 4579.
(39) Reference 15, p 269.
(40) (a) Gunner, M. R.; Tiede, D. M.; Prince, R. C.; Dutton, P. L. In "Function of Quinones in Energy Conserving Systems"; Trumpower, B. L., Ed.; Academic Press: New York, in press. (b) Dutton, P. L.; Gunner, M. R.; Prince, R. C. In "Trends in Photobiology"; Helene, C., Chasier, M., Monteray-Garstier, T., Laustriat, I. G., Eds.; Plenum: New York, 1982; pp 561–70.
(41) Okamura, M. Y.; Isaacson, R. A.; Feher, G. *Proc. Natl. Acad. Sci. U.S.A.* **1973**, *72*, 2251.
(42) (a) Calcaterra, L. T.; Closs, G. L.; Miller, J. R. *J. Am. Chem. Soc.* **1983**, *105*, 670. (b) Miller, J. R.; Calcaterra, L. T.; Closs, G. L. *J. Am. Chem. Soc.* **1984**, *106*, 3047.
(43) Miller, J. R. *Chem. Phys. Lett.* **1973**, *22*, 180; *J. Phys. Chem.* **1975**, *79*, 1070.
(44) Miller, J. R. *J. Phys. Chem.* **1978**, *82*, 767.
(45) Miller, J. R. *Science (Washington, D.C.)* **1975**, *189*, 221.
(46) Miller, J. R.; Beitz, J. V. In "Radiation Research, Proceedings of the Sixth International Congress of Radiation Research"; Okada, S., Ed.; Japanese Association for Radiation Research: Tokyo, 1979; p 301.
(47) Nosaka, Y.; Kira, A.; Imamura, M. *J. Phys. Chem.* **1979**, *83*, 2272.
(48) Kira, A.; Nosaka, Y.; Imamura, M. *J. Phys. Chem.* **1980**, *84*, 1882.
(49) Miller, J. R.; Beitz, J. V. *J. Chem. Phys.* **1981**, *74*, 6746.
(50) Kira, A. *J. Phys. Chem.* **1981**, *85*, 3047.
(51) Huddleston, R. K.; Miller, J. R. *J. Phys. Chem.* **1982**, *86*, 200.
(52) (a) Huddleston, R. K.; Miller, J. R. *J. Phys. Chem.* **1982**, *86*, 1347. (b) *Ibid.* **1983**, *87*, 4867.
(53) Huddleston, R. K.; Miller, J. R. *J. Phys. Chem.* **1981**, *85*, 2992.
(54) Zamaraev, K. I.; Khairutdinov, R. F.; Miller, J. R. *Kinet. Katal.* **1980**, *21*, 616.

$$V(r) = V(R_0) \exp(-(r - R_0)/2a) \quad (3)$$

The attenuated length, a, is typically between 0.5 and 1.0 Å for reactions of radical ions.

The FCWD contains[7-18] the strong dependence of ET rates on reaction exothermicity and on the differences between bond lengths and bond angles in the reactants and products. The FCWD is, in general, strongly temperature dependent, although the temperature dependence may nearly vanish for some reaction exothermicities and in some instances may vanish for all exothermicities at sufficiently low temperatures.

Only those vibrational modes rearranged by the electron transfer need be considered; others just multiply the FCWD by unity. Two types of rearranged vibrational modes are involved:[7-18] low-frequency (<100 cm^{-1}) polarization modes of the solvent and high-frequency (≈500–3000 cm^{-1}) skeletal vibrations of the donor and acceptor molecules. We shall analyze the data in terms of a relatively simple expression based on well-known ET theories[7-18] which incorporate both types of modes.

$$k(r) = (\pi/(\hbar^2 \lambda_s k_B T))^{1/2} |V(r)|^2 \times \sum_{w=0}^{\infty} (e^{-S} S^w / w!) \exp-[(\Delta G^\circ + \lambda_s + w\hbar\omega)^2/4\lambda_s k_B T] \quad (4)$$

The summation in eq 4, which we shall call the "relative Franck–Condon factor", F, contains the dependence of rate on exothermicity (ΔG°) and most of its dependence on the reorganization energies, λ_s and λ_v, which are defined below. The sum is over w, the number of vibrational quanta of the high-frequency vibrations in the product state. $S = \lambda_v/\hbar\omega$ has been called the electron-vibration coupling strength, where ω is the average frequency of the high-frequency modes.

Equation 4 treats the rearranged vibrational modes as displaced harmonic oscillators. The low-frequency modes of the solvent are treated classically, which is appropriate if their frequencies are low ($\hbar\omega << k_B T$). The high-frequency modes are assumed to have a narrow range of frequencies so that several modes can be well represented by an average frequency following methods of Jortner.[12] We then define the reorganization energies

$$\lambda_s = \sum \Delta_i^2 \hbar\omega_i \quad (5a)$$

summed over all solvent modes and

$$\lambda_v = \sum \Delta_i^2 \hbar\omega_i \quad (5b)$$

summed over all high-frequency modes where the reduced displacements $\Delta_i = (\mu_i\omega_i/2\hbar)\Delta R_i$. ΔR_i and μ_i are the displacement in configuration space and the reduced mass for the ith vibration. The ET rate is maximized when the reaction exothermicity equals the total reorganization energy,

$$\lambda = \lambda_s + \lambda_v \quad (6)$$

Equation 4 is a simplified form which neglects frequency changes for reasons explained in the Discussion section, where we will also discuss the adequacy of the classical treatment of the low-frequency modes. This paper will raise important questions about earlier analyses of data on photosynthetic ET to yield information about the nature of those modes. Equation 4 also neglects thermal excitation of the high-frequency modes which is likely to be a reasonable simplification at room temperature and is definitely justified at 77 K.

Equation 4 can be cast in the form

$$k(r) = \nu \exp(-[r - R_0]/a) \quad (7)$$

in which the frequency factor ν contains all the Franck–Condon information

$$\nu = (\pi/(\hbar^2 \lambda_s k_B T))^{1/2} |V(R_0)|^2 F = \nu_0 F \quad (8)$$

where the relative Franck–Condon factor, F, is the sum in eq 4.

If the electron acceptors are distributed randomly and the concentration of donors is much smaller than the concentration of acceptors [D^-] << [A], as in these experiments, then the statistical behavior of all the donors is readily calculated[51] in terms of the (time dependent) effective tunneling radius R:

$$P(t) = \exp[-(4/3)\pi c(R^3 - R_0^3)] \quad (9a)$$

$$R = [(-(3/4)\pi c) \ln P(t) + R_0^3]^{1/3} \quad (9b)$$

$P(t)$ is the surviving fraction of electron donors at time t in the presence of an acceptor concentration c (number per unit volume). Equation 9b is just an inverted form of eq 9a. $k(r)$ is simply related to $P(t)$ via the intermediacy of the tunneling radius R at time t

$$R = R_0 + a \ln (g\nu_0 F t) \quad (10a)$$

$$k(R) = (gt)^{-1} \quad (10b)$$

where the dimensionless constant $g = 1.9$.[51] It is important to note that the ET rate constant as a function of distance in randomly distributed solid solutions is thus obtained from the observable surviving fraction $P(t)$, using only one assumption: that the rate depends strongly on distance. The method will work as long as other factors (e.g., a dispersion of relative orientations or solvation environments) do not become the dominant source of dispersion of ET rates. That is, as long as the distribution of D^-, A pairs peels off in order of distance. The surviving fraction of the donors, P, decays as the tunneling radius, R, grows with time, t. Combining eq 9 and 10 we get

$$P(t) = \exp\left[-\frac{4}{3}\pi c[(R_0 + a \ln (g\nu_0 F t))^3 - R_0^3]\right] \quad (11)$$

which includes the (small) effect of finite size of the reactants and is thus even more accurate than the more complex "exact" result obtained[55] for volumeless point particles. Using eq 9–11 one may obtain the intermolecular ET rate constant as a function of distance using only the assumption of a random distance distribution and the assumption that a strong dependence on donor–acceptor distance determines the distribution of rates. It will be useful later to refer to these (minimal) assumptions and note what conclusions can be drawn from the data without other assumptions.

Equation 11, like the "exact" result, includes ET to all acceptors but neglects hopping among the donor sites ($D_1^- + D_2 \rightarrow D_1 + D_2^-$). Preliminary data indicated hopping to be unimportant[46] and recent, more accurate, data has confirmed this (Beitz, Huddleston, and Miller, unpublished). The reason that hopping is unimportant even at very high concentrations of D, such as [biphenyl] = 0.3 M, is that ET rates are very slow for ET at zero exothermicity in low-temperature glasses, as will be seen below.

The above description, which does not consider F to depend on time, will fail to describe the data presented below. Consideration of time-dependent solvent relaxation known to occur in rigid media allows the model to describe at least all the qualitative features of the data.

We have neglected the effects of molecular orientation on ET rates, because little is known[56] and because the measured $k(r)$ and $R(t)$ values are orientation averaged quantities. An analysis by Zamaraev et al.[57] implies that orientation effects are not large. We agree, however, with the suggestion[56] that the ET rate is likely to decrease an order of magnitude or more for the most unfavorable orientations. However, very few donor–acceptor pairs will have these unfavorable orientations and, for those which do, reactions with second (and farther) nearest neighbors will provide reaction channels so that the observations will be negligibly affected.[51]

II. Experimental Section

Sample preparation and data collection and analysis were described earlier.[38] Briefly, the samples were solutions in 2-methyltetrahydrofuran (MTHF), degassed and sealed under vacuum in 1 × 1 × ≈8 cm boro-

(55) (a) Inokuti, M.; Hirayama, F. *J. Chem. Phys.* **1965**, *43*, 1978. (b) Tachiya, M.; Mozumder, A. *Chem. Phys. Lett.* **1974**, *28*, 87.
(56) Brocklehurst, B. *J. Phys. Chem.* **1979**, *83*, 536.
(57) Doktorov, A. B.; Khairutdinov, R. F.; Zamaraev, K. I. *Chem. Phys.* **1981**, *16*, 351. Zamaraev, K. I. *Sov. Sci. Rev., Sect. B* **1980**, *2*, 357.

Table I. Reaction Exothermicities from Electrochemical Data and Representative Values of the Correction Function Δ_{12} for Each Reaction

compound	abbrev	$-\Delta G°$, eV[a]	ref[b]	correction, Δ_{12}, %[c] 10^{-6} s	10^{2} s	[Bip][d]
biphenyl	Bip	0.0	SS			
2-methylnaphthalene	2MNap	0.010	SS	18.3	10.2	0.3
naphthalene	Nap	0.056	SS	14.0	4.8	0.3
phenanthrene	Phen	0.13	SS	8.3	0.6	0.3
triphenylene	Tri	0.14	SS	2.8	0.7	0.3
2,6-dimethylquinoline	M_2Q1	0.31	TY	2.5	0.1	0.3
biphenylene	Bpln	0.32	SS	1.5	0.0	0.3
7,8-benzoquinoline	BzQl	0.41	TY	1.8	0.0	0.3
triphenylethene	Ph_3Et	0.47	MB	1.5	0.1	0.3
pyrene	Pyr	0.52	SS	1.0	0.0	0.3
fluoranthene	Flth	0.82	SS	1.1	0.0	0.3
acenaphthylene	Acnp	0.95	B	0.7	0.0	0.3
acridine	Acd	1.02	TY	5.6	0.1	0.15
cinnamaldehyde	Cnal	1.08	MB	5.5	0.0	0.3
benzo[*c*]cinnoline	Bcin	1.09	TY	2.0	0.0	0.3
azobenzene	AzBz	1.25	TY	0.6	0.0	0.3
nitrobenzene	NBz	1.4	MB	4.8	0.1	0.15
phenazine	Phenz	1.44	TY	2.2	0.0	0.3
9-fluorenone	Fln	≈1.7	MB	1.4	0.0	0.3
maleic anhydride	MA	1.74	MB	1.0	0.0	0.3
methyl-*p*-benzoquinone	MQ	2.00	P	2.5	0.0	0.3
2-methylnaphthoquinone	MNQ	1.82	P	2.5	0.0	0.3
2,5-di-*tert*-butyl-*p*-benzoquinone	tB_2Q	1.85	P	0.4	0.0	0.3
p-benzoquinone	BQ	2.07	MB	2.0	0.0	0.3
p-dinitrobenzene	DNBz	2.0	MB	2.0	0.0	0.3
2,5-dichlorobenzoquinone	Cl_2Q	2.40	P	2.7	0.0	0.3
tetrafluorobenzoquinone	F_4Q	2.54	P	1.7	0.0	0.3
tetrachlorobenzoquinone	Cl_4Q	2.59	P	2.9	0.0	0.3
tetracyanoethylene	TCNE	2.75	MB	4.0	0.0	0.3

[a] Free energy change for electron transfer from the biphenyl anion to the indicated acceptor in eV. [b] Source of electrochemical data: SS = ref 61; TY = ref 63; MB = ref 58; B = ref 59; P = ref 62. [c] Values at two times for the time-dependent correction, Δ_{12}, for direct capture of trapped electrons by the acceptor. Given in % in A_0 (i.e., % of full scale in Figures 1–5). [d] The concentration of biphenyl in mol/L used in the experiment.

silicate glass cells and frozen to a rigid glass at 77 K. Concentrations of solutes are given in mol/L at 77 K. The concentrations at room temperature were 18% lower. The samples contained a large concentration of a low-electron affinity molecule, usually biphenyl at 0.15 or 0.3 M, and a lower concentration (usually 0.025 M) of a molecule with higher electron affinity.

Frozen samples were placed in a temperature controlled cryostat (Oxford CF 204). Ionization was created in the samples by 20-ns pulses of 15 MeV electrons from the Argonne linac. The ionization produces $\approx 10^{-4}$ M of trapped electrons (e_t^-) and radical cations of MTHF. The cations are rapidly chemically trapped by transfer of a proton to a neighboring solvent molecule. The trapped electrons are stable indefinitely in pure, rigid MTHF but are rapidly ($<10^{-7}$ s) transferred to solute molecules at the high-solute concentrations used (e.g., 0.15 or 0.3 M biphenyl).

The resulting radical anions of the solutes are detected spectrophotometrically over the range 10^{-7}–10^{2} s. The radical anions decay slightly (~3%/decade) over this nine decade time range, due presumably to ion recombination. The presence of a lower concentration of an electron acceptor of higher electron affinity leads to greatly increased decay, accompanied by growth of radical ions of the acceptors. Quantitative measurements of the intermolecular ET are simple when decay of the donor radical ions are observed. Growths of acceptor ions are readily observed but are more difficult to quantitatively correct for the effects of ion recombination for reasons described previously.[49] The data are corrected for overlapping absorptions as described before.[49]

Although the protonation reaction prevents transfer of positive charge from $MTHF^+$ to solutes, at the high concentrations of solutes used, some radical cations of the solutes are formed by direct ionization. In 0.3 M biphenyl in MTHF the yield of biphenyl cations (Bip^+) reaches 10% of the yield of biphenyl anions. The absorption due to Bip^+ was subtracted in some cases. In others this could not be done in a simple way because positive charge transfer to the acceptor occurred. In these cases 0.15 M of a positive charge scavenger was added to remove the Bip^+. Triethylamine (TEA) was suitable positive charge scavenger since TEA^+ does not absorb in the visible region. For acceptors more electron affinic than fluoranthene the 2,2,2-cryptand (sold as Kryptofix 222, E. Merck) was used since TEA might form charge-transfer complexes with the acceptor, whereas the cryptand is sterically hindered. Identical results for Bip^- decay were obtained by using either the method of subtracting away the small Bip^+ absorption or preventing it with a positive charge scavenger.

The data will be presented as ratios A/A_0 of absorbance vs. time in samples with and without the acceptor. Each decay curve is an average of 3–6 accelerator shots per sample, with errors (standard deviations) in A/A_0 being less than ±0.03.

III. Energetic Data for Reaction Exothermicities

Electron-transfer theories[2-21] calculate the nuclear overlap integrals (Franck–Condon factors) as functions of the amount of electronic energy, ΔE (or ΔH since pV terms are generally unimportant), converted to vibrational energy. The best estimates of ΔE are measurements of standard free energy changes, $\Delta G°$, and some recent theories indicate that ΔG should be used.[11,19] $\Delta G°$ can be obtained either directly from equilibria or from closely related electrochemical quantities. Most of the energetic data used here (see Table I) are from polarographic half-wave potentials measured in polar aprotic solvents.[58-65] The differences between the potentials of two compounds may be measured to an accuracy of a few millivolts by the same apparatus, but uncertainties of ≈±0.1 V arise in comparing measurements from different laboratories due to differences in junction potentials, solvents, etc. Additional uncertainties in the actual energy changes in our solid, weakly polar media arise from the fact that the electrochemical measurements are done in polar media. Our earlier study[38] of trapped electron reactions corrected for the polarity change according to the sizes of the acceptors. This was necessarily done in a somewhat arbitrary way.

In the present work we omit such corrections which would change $\Delta G°$ by ≈0.2 eV for some of the highly exothermic re-

(58) Mann, C. K.; Barnes, K. K. "Electrochemical Reactions in Nonaqueous Systems"; Marcel Dekker: New York, 1970.
(59) Bard, A. "Encyclopedia of Electrochemistry of the Elements"; Marcel Dekker: New York, 1978; Vol. XI.
(60) Siegerman, H. In "Techniques of Organic Chemistry"; Weissberger, A., Weinberg, N. L., Eds.; Wiley: New York, 1975; Vol. 5, Part II.
(61) Streitwieser, A.; Schwager, I. *J. Phys. Chem.* **1962**, *66*, 2316.
(62) Peover, M. E. *J. Chem. Soc.* **1962**, 4540.
(63) Tabner, B. J.; Yandle, J. R. *J. Chem. Soc. A* **1968**, 381.
(64) Wiberg, K. B.; Lewis, T. P. *J. Am. Chem. Soc.* **1970**, *92*, 7154.
(65) Szwarc, M.; Jagur-Grodzinski, J. In "Ions and Ion Pairs in Organic Reactions"; Szwarc, M.; Ed.; Wiley: New York, 1974; Vol. 2, Chapter 1.

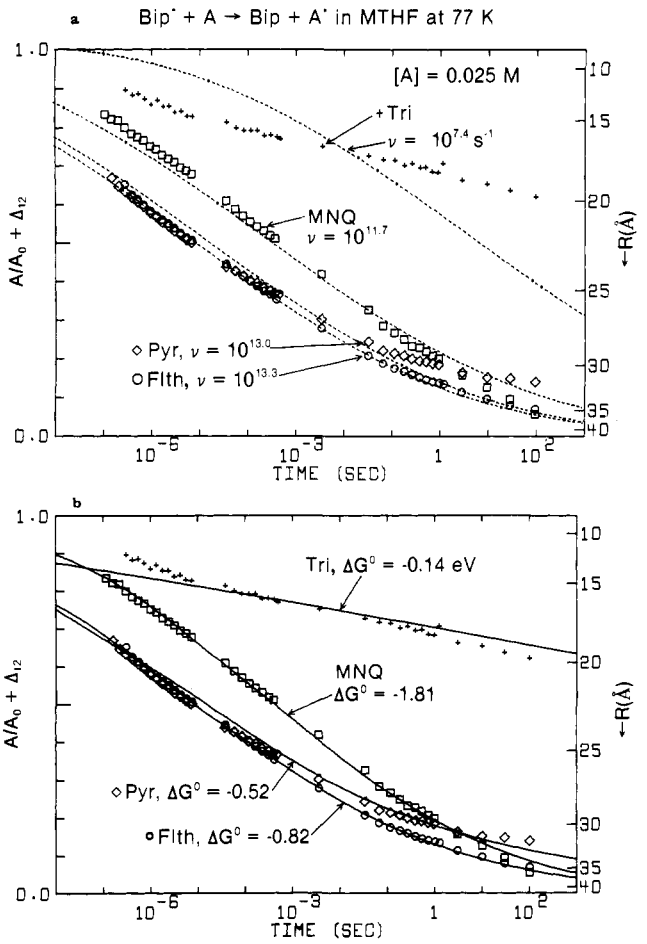

Figure 1. Decay curves giving the fraction ($P = A/A_0 + \Delta_{12}$) of biphenyl radical ions (Bip^-) surviving the intermolecular ET reactions with four different acceptors representative of four regions of reaction exothermicity. A and A_0 are the time-dependent absorbances due to Bip^- in samples with and without the acceptors, and Δ_{12} is a small, time-dependent correction for direct capture of electrons by acceptors. On the right vertical axis one may read the tunneling distances (R) for each reaction as a function of time (see eq 9 and 10). The dashed lines shown in part a are simulations of eq 11, which assumes that each ET reaction has the same exponential dependence of rate on distance and that each reaction has a different Franck–Condon factor, F, which is independent of time. These constant F simulations cannot satisfactorily describe the data for the reactions with pyrene and triphenylene. The more satisfactory solid lime simulations (part b) make F time dependent due to solvent relaxation (see section IVB).

actions (see section V-E). For all the weakly exothermic reactions ($-\Delta G° < 0.5$ eV) where a small error in $\Delta G°$ would have critical importance, we used only acceptors of similar size and nature to biphenyl, so that electrochemical data from polar solvents could be used. Measurements of $-\Delta G°$ for the reaction of the biphenyl anion with naphthalene using electrochemical data in polar solvents[61] ($\Delta G° = -0.056$ eV) and actual measurements of equilibria in less polar THF[65,66] ($\Delta G° = -0.0615$ eV) are in excellent agreement. In the equilibrium work, Szwarc also showed that the entropy change is very small for this electron-transfer process.[65,66] $\Delta G°$ for ET from biphenyl to naphthalene is -0.05 ± 0.01 eV in both MTHF and nonpolar isooctane at 296 K.[42b]

IV. Results

A. Reaction Kinetics of Biphenyl Radical Anions. Reactions of biphenyl radical anions (Bip^-) were followed by measuring the time-dependent concentration of Bip^- by its absorbance, A, at (usually) 650 nm where the molar extinction $\epsilon(Bip^-)650 = 1.1 \times 10^4$ M^{-1} cm^{-1}.[67] The samples contained a large concentration

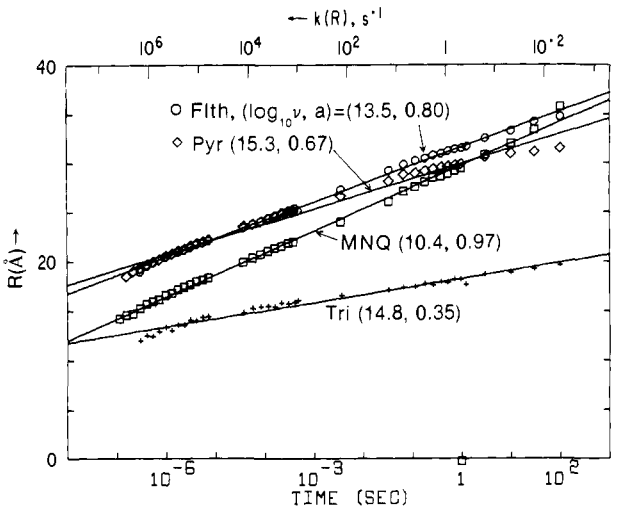

Figure 2. Tunneling distance R as a function of time plotted from the data of Figure 1 using eq 9–10. The plots also give the ET rate constant $k(R)$ as a function of distance using minimal assumptions (see discussion after eq 10 and section V-F). This type of plot is linear if the ET rate is exponential in distance (eq 7). The departure from linearity and the differences in slope for different reactions will be attributed to time-dependent Franck–Condon factors. Parameters a and $\log_{10}\nu$ for the four curves are Flth 0.81, 13.46; Pyr 0.67, 15.29; MNQ 0.97, 10.36; Tri 0.35, 14.84.

of biphenyl (0.15 or 0.3 M) and a smaller concentration of the acceptor. We plot A/A_0 vs. time, where A_0 is the absorbance in a sample which contains the same concentration of biphenyl but no acceptor. A/A_0 measures the fraction of Bip^- ions which have not yet transferred their electrons to acceptors at time t. The data presented herein contain small corrections for absorbance of the radical anion of the acceptors and for direct capture of trapped electrons by the acceptors. The nature of the small correction for direct capture by acceptors, Δ_{12}, is briefly described at the end of this section. The corrected A/A_0 plots presented thus directly relate electron-transfer distance, R, to time (eq 9) and thus obtain the (orientation averaged) ET rate constant $k(r)$ as a function of distance (eq 7–10).

Actual decay curves are presented here for about half the reactions studied; the other half appear in supplementary material. The data shown herein are representative of all the data, giving equal play to decay curves fit well or fit poorly to the kinetic model presented below.

Figure 1a shows decay curves ($A/A_0 + \Delta_{12}$ plots) for four reactions representing a range of exothermicities, $-\Delta G°$, from 0.14 eV (triphenylene) to 1.81 eV (2-methylnaphthoquinne). It is apparent that the biphenyl anion reacts most rapidly with pyrene ($-\Delta G° = 0.52$ eV) and fluoranthene (0.82 eV): The reactions with intermediate exothermicities are fastest. The dashed line simulations are plots of eq 11 with $\nu = \nu_0 F$ chosen to give the best fit to each decay curve, while requiring that all the reactions have the same dependence on distance. The determination of a, which specifies the distance dependence, is described in the Discussion section. This distance dependence ($a = 0.83$ Å) fits well the data for the fastest reaction (with fluoranthene). But it is apparent that the data for the other acceptors cannot be fit by simply choosing a different F for each acceptor. The more adequate solid line simulations in Figure 1b make F time dependent due to solvent relaxation processes according to a simple model described in the Discussion section.

Figure 2 plots $R(t)$, the time-dependent "tunneling distance" or "reaction radius". Figure 2 just replots the data of Figure 1, making use of eq 9b, which directly relates $R(t)$ to the surviving fraction of Bip^-, $P(t) = A/A_0 + \Delta_{12}$, assuming only a random distribution of acceptor molecules and a rapid falloff of rate with distance.

(66) Karasawa, Y.; Levin, G.; Szwarc, M. *Proc. R. Soc. London, Ser. A* **1971**, *326*, 53.

(67) Shida, T. In "Advances in Radiation Research"; Duplan, J., Chapiro, A., Eds.; Gordon and Breach: New York, 1972; Vol. 2, p 483.

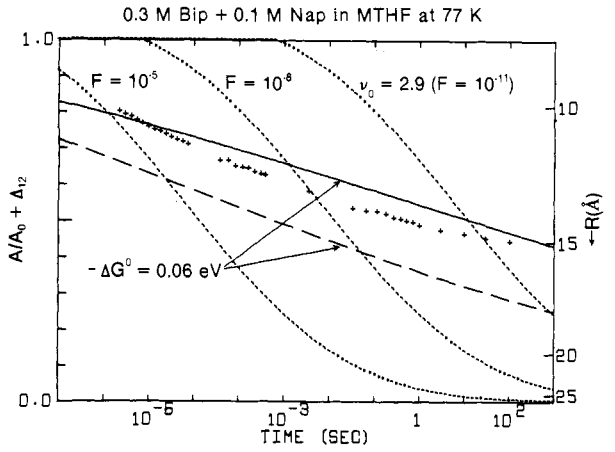

Figure 3. Reaction of the biphenyl anion with 0.1 M naphthalene. The three constant F simulations of eq 11 (short dashes) contrast sharply with the observed decay curve. The two simulations of the solvent relaxation model assume that λ_s does not depend on the distance between the reactants (solid line) or that λ_s has the full distance dependence of a fully relaxed dielectric continuum (eq 13).

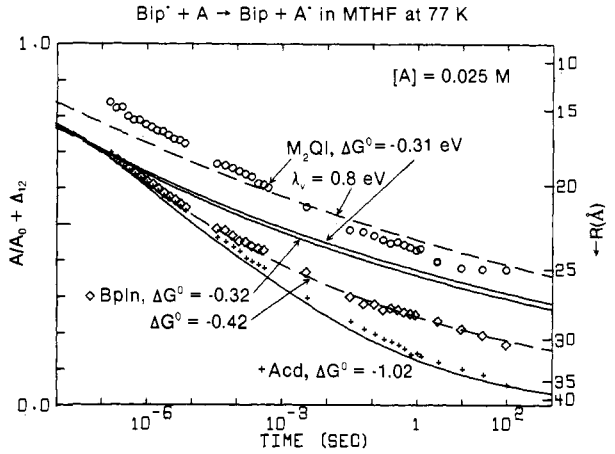

Figure 4. Decay curves for reactions of the biphenyl anion with acridine, biphenylene, and dimethylquinoline. Simulations using the solvent relaxation model (solid lines) and $\Delta G°$'s from published electrochemical measurements decay too fast for M_2Q1 and too slow for Bpln. A larger λ_v leads to a reasonable fit for M_2Q1 (dashed line). Only by adjusting $\Delta G°$ can the Bpln data be fit by the model.

An advantage of the tunneling distance plot is that it gives a straight line (eq 10a) of slope a ln 10 if the ET rate depends exponentially on distance (eq 7) and F does not depend on time or distance. A linear plot is obtained for the reaction of the biphenyl anion with fluoranthene. Plots for the other reactions have different slopes. The plot may also be read to give the ET rate constant $k(r)$ (upper horizontal axis) as a function of r using eq 10b.

The weakly exothermic and therefore slow reaction of Bip^- with naphthalene (Figure 3) was measured with a high concentration of naphthalene (0.1 M) to obtain a substantial amount of decay. Figures 4 and 5 show data for reactions not well fit by the relaxation model unless some parameter is taken as adjustable. These include all the very highly exothermic reactions ($-\Delta G_0 >$ 2.1 eV). Section V-E discusses these results.

In the figures a correction, Δ_{12}, has been added to A/A_0 to account for the direct capture of trapped electrons by acceptors. If biphenyl and the acceptor molecules capture electrons with equal efficiency, then the fraction captured directly by the acceptor would be the concentration ratio [A]/([Bip] + [A]) = 0.143 or 0.077 for 0.15 or 0.3 M Bip + 0.025 M acceptor.

The correction, Δ_{12}, is always less than [A]/([Bip] + [A]) and generally decreases with time due to correlation between probabilities of competition and intermolecular electron transfer. The method for making this correction has been described in detail

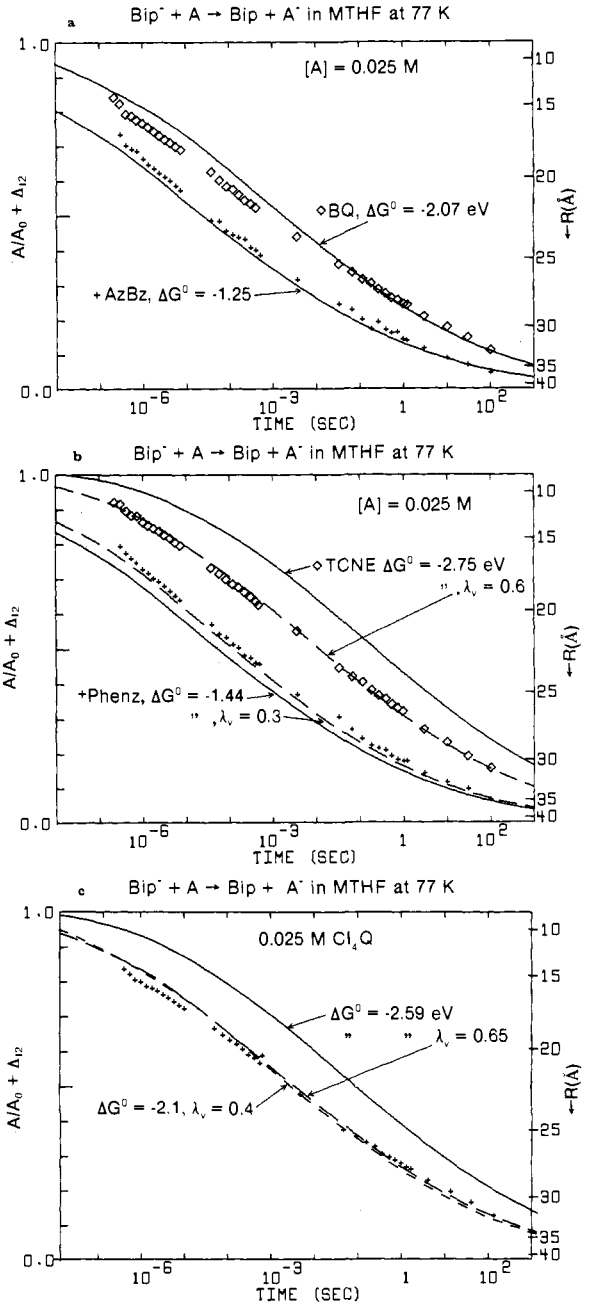

Figure 5. Decay curves for reactions which are showed by high exothermicity. For reaction with TCNE and Cl_4Q (5b and 5c), the simulations of the solvent relaxation model with the standard parameters do not fit well, but reasonable fits (dashed lines) can be obtained by adjusting one parameter (see text).

and tested.[52] It requires separate measurement of kinetics of trapped electron reactions as in ref 38. Values of the correction, Δ_{12}, are given at two times (10^{-6} and 10^2 s) each reaction in Table I. Δ_{12} is as large as 19% of A_0 for the slowest reaction but is more typically ≈5% of A_0 at 10^{-7} s, decreasing to less than 1% by 1 s.

B. Reactions of Other Donors. To assess whether the biphenyl anion might be somehow unusual, we measured highly exothermic reactions of the biphenyl, fluorene, naphthalene, phenanthrene, and triphenylene anions with an acceptor, 0.025 M methyl-*p*-benzoquinone. The decay curves (see supplementary material) were all similar, but showed an increase in rate with decreasing exothermicity as expected. The behavior of the biphenyl anion is typical.

V. Discussion

The principal questions to be answered are how do ET rates depend on distance and reaction exothermicity? If each reaction

Table II. Common Parameter Set

parameter	value	how obtained
Distance Dependence $k(r) = \nu_0 F \exp[-(r - R_0)/a]$		
a	0.83 Å	curve through fastest reactions
$\nu_0(R_0)$	$10^{13.9}$ s^{-1}	at each time; overall fastest reactions
Energy and Time-Dependent Franck–Condon Factors		
$\lambda_s(10^6$ s)	0.4 eV	peaks of $\Delta G°$ vs. rate curves
$q \equiv d\lambda_s/d \log t$	0.045 eV/decade	fits of reactions with small $-\Delta G°$
λ_v	0.4 eV	peaks of $-\Delta G°$ vs. rate curves
$\hbar\omega$	1500 cm^{-1}	spectroscopy, crystallography

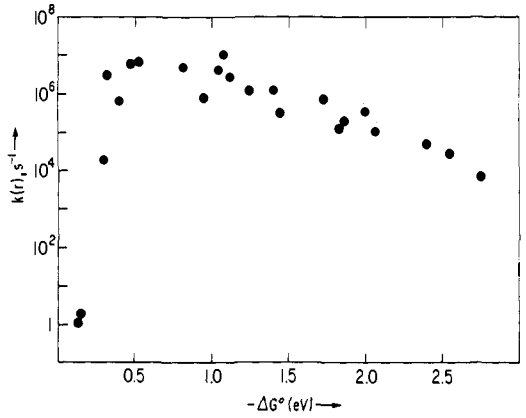

Figure 6. ET rate constant $k(r)$ for r = 18 Å plotted vs. $\Delta G°$. Making this plot requires no assumptions about the distance dependence of ET rates (the parameter a). But this plot is very misleading because the rates at the same distance are measured at greatly different times, when λ_s is different (see text).

differed from the others only by having a different (but time independent) Franck–Condon factor, F, in eq 8–10, then the data would have been fit by the short dashed line simulations in Figures 1 and 3. Furthermore, decay curves for reactions with different acceptors compared at the same concentration would have been parallel: the decay curve for one reaction could have been superimposed onto that for another by translation along the log t axis by the amount log (F_1/F_2). The data do *not* show this parallel behavior; the situation is clearly more complicated.

Better fits can be obtained by allowing both F and the range parameter, a, to vary freely (see Figure 2 for examples). But in the data presented here, $\Delta G°$ is changed by changing only the acceptor, and calculations of electron exchange matrix elements, $V(r)$, suggest that the range parameter a should be almost invariant to changes in electron affinity of the acceptor (see section C below).

We will show that the complicated behavior of the data can be well understood by requiring the Franck–Condon factors, F, to become time dependent due to time-dependent solvent relaxation around the transient electron donor (e.g., the biphenyl anion radical ion). In the model to be presented below (section V-B) ν_0 and a are fixed (identical for all acceptors reacting with the same donor), while F depends on time in a way determined solely by the reaction exothermicity, $-\Delta G°$. This model gives reasonably good fit to the data (see solid lines in Figures 1–5). Table II gives the common set of parameters used to calculate the biphenyl anion reactions with all acceptors using eq 4, 11, and 14.

We advocate a model which considers individual variations in reorganization energies for each donor and acceptor, which would provide better fits. But until more data are available, adjusting reorganization energies for each acceptor would be an underdetermined procedure. At present we suppress individual variations in solvent reorganization energies to demonstrate dominance of a more important factor, the time dependence of λ_s. The motivation for this view is most apparent when we plot rate vs. exothermicity at different times. In some cases the reorganization energy of skeletal vibrations, λ_v, will be adjusted to show that

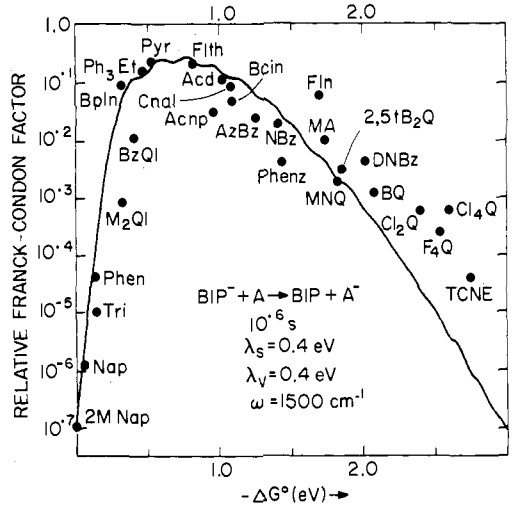

Figure 7. Relative rates of ET reactions of the biphenyl anion as a function of exothermicity at 10^{-6} s expressed as relative Franck–Condon factors (see eq 4, 10, 11, and 12). The line was calculated by using eq 4.

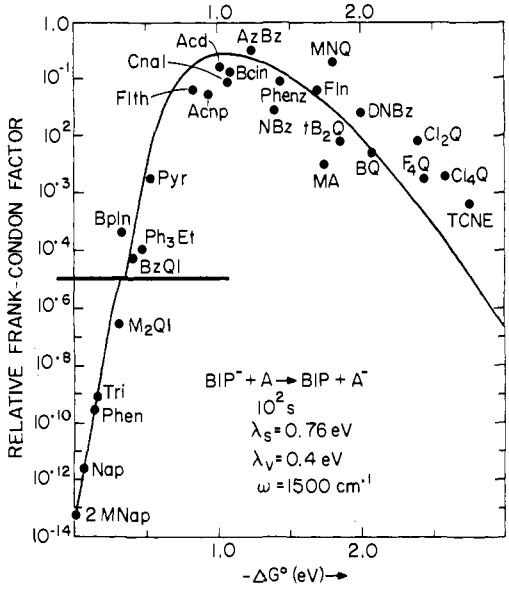

Figure 8. Relative rate vs. exothermicity for the same reactions shown in Figure 7 but observed at 10^2 s. The vertical axis is compressed below 10^{-5}. The calculation of the solid line is the same as in Figure 7, except that λ_s is increased to 0.76 eV.

plausible variations of this one parameter can account for variations of some reactions.

A. ET Rate as a Function of Reaction Exothermicity. Figure 6 plots $k(r)$ for r = 18 Å using eq 9–10. Physically the plot is just the reciprocal of $1.9t$, where t is the time necessary to reduce the surviving fraction of donors (Bip^-) by the amount corresponding to disappearance of all D^-, A pairs at $r \leq 18$ Å. This plot requires few assumptions (see assumptions for eq 9–11) but is probably quite misleading because it compares different reactions measured at very different times, which is inappropriate if Franck–Condon factors are strongly time dependent. We believe the plots of Figures 7 and 8 below give a much better measure of ET rate as a function of reaction exothermicity with other variables held constant (see Discussion).

Figures 7 and 8 plot ET rate vs. reaction exothermicity $-\Delta G°$ (see Table I for values) at two different times, 10^{-6} and 100 s. The points plotted in Figures 7 and 8 were obtained from the data of Figures 1–6 using eq 9–11 in a way described later in this section. Figures 7 and 8 have notable differences. At 10^{-6} s (Figure 7) an exothermicity of $\approx$0.8 eV maximizes the ET rate, but $\approx$1.1 eV is required to maximize the rate at 100 s. A plot

at an intermediate time (10^{-2} s) peaks at an intermediate energy (see supplementary material). This implies that the total reorganization energy $\lambda = \lambda_s + \lambda_v$ is larger at longer times. The 100-s plot is also broader, and the weakly exothermic reactions (e.g., $Bip^- + Nap$, $-\Delta G° = 0.06$ eV) are slowed by many more orders of magnitude. These observations are compatible with an increase in λ with time due to an increase in λ_s, the solvent reorganization energy. The solid lines in Figures 7 and 8 fit the rate vs. $\Delta G°$ plots using eq 3 making just that assumption: The curve drawn on the plot for 100 s is the same as that for 10^{-6} s except that λ_s is increased from 0.4 to 0.76 eV. The reorganization energy ($\lambda_v = 0.4$ eV) and average frequency (1500 cm^{-1}) for the skeletal vibrations were estimated from spectroscopic, crystallographic, and MO calculations collected by Fischer and Van Duyne for the reaction of the naphthalene anion with TCNQ.[9]

Within the context for the model of eq 4 the increase of λ_s with time can be regarded as an experimental finding. The ET rates must be maximized at $-\Delta G° = \lambda = \lambda_s + \lambda_v$, and the data are fit well (Figure 8) by assuming an increase in λ_s but not by assuming an increase in λ_v. If λ_v, not λ_s, were increased to match the peak in Figure 8, the weakly exothermic ($0 < -\Delta G° < 0.5$ (eV)) reactions would be barely affected: eq 4 gives a curve (not shown) only slightly below that in Figure 7 for the $0 < -\Delta G° < 0.2$ (eV) region. The data (Figure 7), by contrast, show a very large decrease in the relative rates of the weakly exothermic reactions. There is also a physical basis for the increase of λ_s with time, as described in the next section.

Next we consider the method for obtaining the plots of Figures 7 and 8 from decay curves given in Figures 1–6. We chose to compare rates of the different reactions *at the same time*. The reaction radii $R_1(t)$ and $R_2(t)$ for two reactions were obtained from the decay curves using eq 9. Then eq 11 gave the relative Franck–Condon factors for the two reactions as

$$F_2/F_1 = \exp[R_2(t) - R_1(t)]/a \qquad (12)$$

The plots of Figures 7 and 8 therefore depend on the assumption that a does not depend on $\Delta G°$. This assumption seems very likely to be correct (see section C). It (or some information about a) is necessary to obtain Franck–Condon factors from the measured ET rates so that the data may be quantitatively interpreted in terms of ET theories.

No assumption about a is necessary for the central qualitative conclusions of this paper (1) that the tunneling distance $R(t)$ and therefore the ET rate constant k are maximized for an intermediate exothermicity and (2) that the exothermicity needed to maximize the rate gradually increases with time from $\approx$0.8 eV at 10^{-6} s to $\approx$1.1 eV at 10^2 s. If $R(t)$ were plotted instead of F in Figures 7 and 8, the maxima would occur at the same $\Delta G°$'s. Even if a were hypothesized to vary with $\Delta G°$, no systematic dependence of a on $\Delta G°$ could cause the $\Delta G°$'s which maximized the ET rate to shift with time. We conclude that the only plausible explanation for the shift of the peaks in Figures 7 and 8 is an increase of λ with time.

The values of F plotted in Figures 7 and 8 are referenced to $F = 1$. All points fall below this value since F, as we defined it, is unity only for $\Delta G° = -\lambda_s$ and $\lambda_v = 0$. This ideal, $F = 1$, reaction would have a rate constant following eq 7 with $\nu = 10^{13.9}$ s^{-1} and $a = 0.83$ Å (see section V-C).

Another method is to fit each decay curve to eq 10a allowing both $\nu = \nu_0 F$ and a to vary to obtain the best fit. This method gives good fits to the data (see Figure 2 for examples). The ν vs. ΔG_0 plot (see Figure S-7 in the supplementary material) rises steeply to a maximum at $\Delta G_0 \cong 0.15$ eV and then falls by 7 orders of magnitude. The range parameter a gradually increases with exothermicity from $a = 0.19$ to 0.96 Å. We believe that parameters ν and a obtained this way are simply an exercise in curve fitting and have no physical meaning (see below).

ET rates for hole-transfer reactions in glassy matrices were measured as a function of exothermicity by Kira.[50] He saw no significant decrease of rate at high exothermicities. This may indicate important and interesting differences between hole-transfer and electron-transfer reactions. However, that data must be treated with caution. The only highly exothermic reactions in that study involved the matrix trapped hole, thought to be 2-chlorobutane cation ($2CB^+$). From photoelectron spectra, we must expect (1) a much larger reorganization energy, λ, for this σ cation than for π systems and (2) that electronically excited products will lower the effective exothermicity of reactions with dimethylaniline. Because the absorption band assigned to $2CB^+$ is overlapped by another species, it is not clear how kinetics of $2CB^+$ were accurately measured. Furthermore, the reactions in ref 50 were not reactions of a common donor with several acceptors, as in the present work. Both ν and a are therefore *expected* to change for the different reactions. The dependence of a on the energetics of these hole-transfer reactions is complicated and not well understood.[46-50]

B. Molecular Relaxation and Time-Dependent Franck–Condon Factors. The increase of the solvent reorganization energy, λ_s, with time can be associated with a definite physical mechanism: that of dielectric relaxation by reorientation of solvent molecules around a charge added suddenly to a molecule in a solid. This process leads to dynamic spectral shifts,[68-71] which have been observed[70,71] to have kinetics extending over our entire time range of 10^{-7} to 10^2 s in glassy solvents such as ethanol and MTHF at 77 K. The amount of spectral shift is almost linear in log t over this range, reflecting a dielectric polarization which relaxes toward equilibrium with a wide range of dielectric relaxation times.

The spectral shifts are apparently closely related to electron-transfer processes: Only those transitions which substantially redistribute charge in the molecular ions give rise to substantial spectral shifts. For example, the transition in the benzophenone radical ion which removes electron density from the carbonyl[72] and places it on the rings shifts substantially,[68-70] and the shift is larger in more polar solvents. Anions of aromatic hydrocarbons such as biphenyl show only very small shifts as expected, since the optical transitions in these ions do not greatly alter the charge distribution.

The close connection between solvent polarization and solvent reorganization energies is illustrated in the expression[2] for λ_s in a dielectric continuum

$$\lambda_s = -e^2\left(\frac{1}{2r_D} + \frac{1}{2r_A} - \frac{1}{R_{DA}}\right)\left(\frac{1}{\epsilon_s} - \frac{1}{\epsilon_{op}}\right) \qquad (13)$$

where r_D and r_A are radii of the donor and acceptor, R_{DA} is the donor–acceptor distance, and ϵ_s and ϵ_{op} are the static and optical dielectric constants. Our key assumption will be that the dielectric is not fully relaxed around an injected charge (e.g., to create biphenyl anion). Then ϵ_s in eq 13 is replaced by a time-dependent quantity $\epsilon(t) \leq \epsilon_s$, and λ_s becomes time dependent. Dielectric spectroscopy[73-76] has shown that ϵ is generally time dependent in solids, although the effective $\epsilon(t)$ we need would not be measured by dielectric spectroscopy since the large electric fields near the ions will certainly accelerate relaxation processes. This difficult problem was neglected in a theory attempting to connect dielectric relaxation to electron transfer in polymers.[21]

A fully correct description of the findings of this paper would require more direct experimental information than given by the spectral shifts cited above and a new theory to incorporate the time-dependent effects. Both are beyond the scope of this paper. It is useful to show that a semiempirical description which retains

(68) Hoshino, M.; Arai, S.; Imamura, M. *J. Phys. Chem.* **1974**, *78*, 1473.
(69) Baxendale, J. H.; Atherton, S. J.; Hoey, B. M., private communication.
(70) Huddleston, R. K.; Miller, J. R. *Radiat. Phys. Chem.* **1981**, *17*, 383.
(71) Huddleston, R. K.; Miller, J. R. *J. Phys. Chem.* **1982**, *86*, 2410.
(72) See the molecular orbital analysis in: Shida, T.; Iwata, S.; Imamura, M. *J. Phys. Chem.* **1974**, *78*, 741.
(73) Shablakh, M.; Hill, R. M.; Dissado, L. A. *J. Chem. Soc., Faraday Trans. 2* **1978**, *78*, 625, 639. Johari, G. P. *Ann. N. Y. Acad. Sci.* **1976**, *279*, 117.
(74) Wong, J.; Angel, C. A. "Glass Structure by Spectroscopy"; Dekker: New York, 1976.
(75) Williams, G. *Trans. Faraday Soc.* **1966**, *62*, 2091.
(76) Johnscher, A. K. *Phys. Thin Films* **1980**, *11*, 205.

the simple form of eq 4 can account, in at least a qualitative way, for all the unusual features of the data.

Previous ET theories[2-19] were principally concerned with reactions in fluid solutions, where dielectric relaxation around transiently produced reactants could be assumed to be complete. In solids, however, dielectric relaxation is often incomplete on any practical time scale, and a large range of dielectric relaxation times is typically found which is broader than the time range of the measurements in this work.[73-76] In such a situation, it is readily shown that the amount of dielectric relaxation and the solvent reorganization energy, λ_s, will vary approximately as log t over some time range

$$\lambda_s(t) = \lambda_s(t_0) + q \log (t/t_0) \qquad (14)$$
$$t_0 \leq t \leq t_f$$

where $q = d\lambda_s/d(\log t)$ would be a slowly varying function of log t for the kinds of dielectric responses typically observed in disordered solids. In the absence of any direct measurements of $\lambda_s(t)$, we empirically determine $\lambda_s(t)$ from the maxima of plots such as Figures 7 and 8 (see also supplementary material). The simplest form which represents the movement of this maximum with time is eq 14 with constant q. The value of this constant is $q = (0.76 - 0.4)/8$ decades = 0.045 eV/decade. This empirical form is consistent with the fact that the amount of dynamic spectral shifts[68-71] is close to linear in log t. We shall use this empirical description of the movement of the maxima of the F vs. $\Delta G°$ plots to see if a reasonable description of the ET kinetics, even for $\Delta G°$'s far from the maxima, can result. We might expect this description to fail since the physics which could lead to eq 14, such as double well potentials (for each diabatic surface—the adiabatic surface for ET would have four minima) or use of frictional terms, may be inconsistent with the treatment of the solvent in eq 4. In the absence of any appropriate theory, it is useful to test the simplest possible assumption that $\lambda_s(t)$ from eq 14 may be inserted into eq 4.

With this assumption, the vast ($>10^{12}$) range of relative rates and the different shapes of the decay curves are given in one common description using eq 4, 8, 11, and 14. In this description the only parameter varied from one reaction to another is the exothermicity $-\Delta G°$, but in a few cases adjustment of λ_v is also considered. Simulations of this description are compared with experimental decay curves in Figures 1b and 3–5. The ability of this model to represent the data is evaluated in comparison to other procedures in section E below.

Unusual effects of temperature are expected from the above mechanism. Increasing temperature increases solvent relaxation rates so that λ increases more rapidly with time. For weakly exothermic reactions $d\lambda/dT > 0$, leading to a diminished *apparent* activation energy, which can even become zero or negative. Preliminary experiments on the reactions of the biphenyl anion with naphthalene and phenanthrene showed apparent *negative* activation energies (see Figure S-10). Such effects can occur only when medium relaxation effects compete with ET and will therefore not be important in fluids except at very short times. The sharp disappearance of thermal activation for ET from cytochrome *c* to chlorophyll in *Chromatium*[20] could be due to relaxation of the environment around the chlorophyll cation. If an important relaxation process becomes competitive with ET at ≈100 K, this mechanism may be an attractive alternative to the enormous change in a ≈400-cm^{-1} metal ligand vibrational mode[12] which has never been confirmed but is required by most theoretical treatments[12,14-16,20] (see ref 19 for an exception).

The above represents a simplified treatment of ET rates when solvent relaxation is time dependent for both the reactants and products. Van Duyne and Fischer provided an interesting treatment of ET reactions with fully relaxed reactants but slow solvent relaxation in the products.[8]

Our reviewers have pointed out that it may be useful to consider that slow relaxations may cause ΔG (or perhaps an effective ΔG) as well as λ_s to change with time. The very simple treatment presented here does not admit adjustments of ΔG. We define ΔG such that $\Delta G = 0$ at all times for an exchange reaction $D_1^- + D_2 \rightarrow D_1 + D_2^-$, where D_1 and D_2 are identical molecules (except that D_1 initially has the electron and has polarized the surrounding medium). Defining an effective, more positive, ΔG will require division of solvent relaxations into "fast" and "slow" processes. This division may be arbitrary and will encounter the difficulty that all solvent relaxations are possible in principle, given enough time.

Until now we have neglected the *distance* dependence of λ_s predicted by the equilibrium dielectric continuum expression, eq 13. λ_s may actually depend much more weakly on distance than eq 13 suggests, because the solvent polarization around ions created in rigid matrices may be very local if reorientation of solvent molecules is driven primarily by the high electric field of the ion.

We attempted an experimental test of the effect of distance on λ_s with inconclusive results. The expected (by eq 13) effect of distance on λ_s is large only at short reaction distance (≤10 Å). Reactions at these short distances occur within our time range only for the slowest reactions. The very weakly exothermic reactions observed in Figure 3 and Figure S-1 (supplementary material) this provide the best test case, especially since these slow reactions are very sensitive to the small changes in λ_s given by eq 13. The simulations in Figure 3 which omit (solid line) or include (long dashed lines) the distance dependence of eq 13 differ, but the data fall between the two types of simulations. This could be taken to indicate that λ_s does depend on distance, though more weakly than predicted by eq 13, as the above reasoning suggests.

When both reactants are ions, electrostatic effects give an additional dependence of ET rates of distance.[77,78] They are negligible in the present case where the electron acceptor is always neutral.

C. Distance Dependence of Electron Exchange Interactions. Two theoretical methods for describing the behavior of electron exchange interactions, $V(r)$, at long distances are available, and both lead to the same conclusion: the range parameter a in eq 3 should be almost invariant for reactions of a common electron donor with different acceptors having greatly different electron affinities. The simplest method is to calculate $V(r)$ for simple double well potentials (e.g., δ functions and square well or double Coulomb potentials). Redi and Hopfield[14c] obtained the usual result that a varies as $B^{-1/2}$, where B is the binding energy of the electron on the electron *donor*. It is implicit in their treatment that the parameter a does not depend on the nature of the acceptor because for thermal ET the donor only interacts with states of the acceptor at the same energy. Redi and Hopfield also considered optical ET,[14c] where electronic energies of the donor and acceptor are different. At long distances ($r - R_0 \gg a$), $V(r)$ is dominated by the term for the more shallowly bound level, which for thermal ET is the donor. Thus, there are two reasons why the parameter a should depend on the donor, with negligible dependence on the acceptor. At very short distances a decreases slightly for highly exothermic reactions—opposite to the trend seen in our data if a is allowed to vary to obtain fits.

Superexchange models of $V(r)$[17,49] were found to provide a better description of ET involving positive ions.[49] Superexchange models assume that direct exchange between the donor and acceptor is small compared to indirect interactions coupled through electronic states of the intervening solvent. $V(r)$ is still an exponential function of distance, but the range parameter a varies as $(\ln B)^{-1}$ instead of $B^{-1/2}$, where B is the energy required to remove an electron from the donor and place it in the solvent.[49] Individual characteristics of the acceptor affect only the last element in a chain of interactions and can therefore affect only the preexponential factor but not the distance dependence of $V(r)$. We, therefore, assume a to be independent of the nature of the acceptor, even though adjusting a can improve fits to the data.

Other viewpoints have been expressed. Decay curves observed[43] for reactions of trapped electrons with acceptors have been in-

(77) Van Leeuwen, J. W.; Heijman, M. G. J.; Nauta, H.; Casteleijn, G. *J. Chem. Phys.* **1980**, *73*, 1483. Van Leeuwan, J. W.; Levine, Y. K. *Chem. Phys.* **1982**, *69*, 89.
(78) Rice, S. A.; Pilling, M. J. *Prog. React. Kinet.* **1978**, 9, 93.

Table III. Electron Exchange Matrix Elements $V(r)^a$ Measured as a Function of Distance[b] r

r, Å	$V(r)$, eV	r, Å	$V(r)$, eV
6	3.9×10^{-2}	30	2.1×10^{-8}
10	3.5×10^{-3}	35	1.0×10^{-9}
15	1.7×10^{-4}	50	1.2×10^{-13}
20	8.5×10^{-6}	75	3.5×10^{-20}
25	4.2×10^{-7}	100	1.0×10^{-26}

[a] The values are averaged over angular orientation and have been measured only in the range 15–35 Å. [b] The center-to-center distance from the biphenyl anion to the acceptor.

terpreted[77-79] by adjusting a, although no theoretical justification has been offered for this procedure. This paper provides an alternative explanation which is physically sensible and compatible with the data.

If a is constant for reactions of one donor with several acceptors, we can determine its value. Rate vs. distance data for an ET reaction cannot be simply fit to an exponential to yield the range parameter, a, because time dependent Franck–Condon factors also shape the decay curve. This shaping effect can be eliminated by using data for all acceptors: ET rates are optimized (F approaches unity) at $\approx 10^{-6}$ s for reactions having $-\Delta G^\circ = 0.5$–0.8 eV. The rates are optimized at 10^2 s for $-\Delta G^\circ \approx 1.2$ eV. We used all the data for reactions with $0.5 \leq -\Delta G^\circ \leq 1.4$ (eV) to eliminate Franck–Condon effects to obtain the electron exchange matrix element as a function of distance yielding $a = 0.83$ Å and $V(R_0 = 6\ \text{Å}) = 0.039$ eV. Table III gives values for $V(r)$ at various distances, including estimates which go beyond our actual range of measurements. $V(r)$ can also be obtained nearly as well from data for one reaction of intermediate exothermicity. Fitting the data for the biphenyl anion + fluoranthene reaction ($\Delta G^\circ = -0.82$ eV) gives $a = 0.81$ Å. Measurements of fluorescence quenching have yielded $a = 0.7$ Å.[80] An ab initio calculation[11] of $V(r)$ for the Fe(III)/Fe(II) exchange reaction in water gave the value $a \cong 0.55$ Å. We may speculate that this faster decrease of $V(r)$ is a result of the larger binding energy, B.

D. Effects of Frequency Changes. An extensive analysis of spectroscopic and crystallographic data by Fischer and Van Duyne[9] showed that most of the bond length changes for the reaction of the naphthalene anion with TCNQ were in vibrational modes with frequencies near 1500 cm^{-1}. Redoing their calculations, but neglecting frequency changes, we found a rate vs. ΔG° curve only slightly different from theirs. This justifies the simple form of eq 4, which neglects frequency changes, and considers bond length changes in a group of modes close enough in frequency to be represented by an average. Webman and Kestner[7b] reached a similar conclusion.

The present data could not be fit to meaningfully extract both bond length and frequency changes, and highly sophisticated treatments are not justified. Including frequency changes of the magnitude calculated by Fischer and Van Duyne[9] would have increased calculated rates in the highly exothermic region, with little effect on the rest of the curve. This would improve agreement of theory with experiment.

E. ΔG° and λ as a Function of the Nature of the Acceptors: Limitations of the Data and Evaluation of the Relaxation Model. Polarization energies for radical anions are sensitive to both size and charge distribution within the ion. For example, the benzoquinone anion (BQ) will have a larger polarization energy than the biphenyl anion because BQ's π system is smaller and because the charge is concentrated on the oxygens. These differences lead to larger λ_s for reactions of quinones and nitriles than for reactions of polycyclic aromatic hydrocarbons. Because our most exothermic reactions involve quinones and nitriles, there is some bias in our ΔG° vs. rate plots (Figures 7 and 8). Furthermore, we add to this bias by slightly overstating the exothermicity of the highly exothermic reactions for two reasons: (1) The reduction potentials are measured in highly polar solvents containing electrolytes, conditions which favor reduction of molecules such as BQ relative to larger π systems such as biphenyl, naphthalene, or pyrene. (2) The strong acceptors form donor–acceptor complexes[81,82] with the solvent, MTHF, which almost certainly decrease their electron affinities. These effects, taken together, probably decrease $|\Delta G^\circ|$ by less than 0.4 eV for even the most exothermic reactions, but we made no corrections to the ΔG°'s, since the size of these corrections is only approximately known. To minimize the errors in ΔG° due to solvent polarity we follow ref 38 in using acceptor molecules with reasonably delocalized charge distributions. The ΔG°'s estimated from gas-phase electron affinities for the quinones and TCNE differ by less than 0.3 eV from the ΔG°'s in Table I.

Both of the above factors tend to make observed rates of highly exothermic reactions faster than expected assuming a constant λ for all acceptors and using ΔG°'s obtained in more inert and polar solvents, such as acetonitrile. The observed decay curves would also be expected to be steepened but not as much as expected if the time independent part of λ_s were larger for the highly exothermic reactions. The observations do depart from calculated curves in just this way for highly exothermic reactions. This departure can be interpreted to mean that for highly exothermic reactions rate vs. ΔG° falls less steeply than expected from the location of the peak of the rate vs. ΔG° plot, since we used these peaks to determine λ.

The fits of the relaxation model to very highly exothermic reactions can always be improved by using an exothermicity smaller than published values (see Figure 5). Similar improvements are obtained by increasing λ_v (Figures 5, S-5, and S-6). In fact, all of the very highly exothermic reactions can be fit well either by increasing λ_v, decreasing exothermicity, or a combination of both, while both are physically plausible. Bond length and angle changes are likely to be larger in the strong acceptors where electron withdrawing groups concentrate charges. This was illustrated in Fischer and Van Duyne's analysis of the naphthalene anion, TCNQ reaction where TCNQ contributed much more to λ_v than did naphthalene.[9] There are also examples of weakly exothermic reactions (M_2Q1, BzQ1) for which increased λ_v (compared to 0.4 eV) give improved fits, and other cases where decreased values of λ_v give improved fits (Phenz, Bpln, AzBz). These cases may truly measure different amounts of bond length and frequency changes when those molecules are converted to anions, but independent corroboration is very desirable. Even so, quantitative measurements of λ_v from this data for highly exothermic reactions would require quantitative measurements of the corrections to ΔG° mentioned above.

The accomplishments of the relaxation model are that it predicts all the qualitative features of the data, including (1) the severe flattening of decay curves for weakly exothermic reactions, (2) the flattening of decay curves for moderately exothermic reactions (e.g., pyrene) only at long times, (3) the slight steepening (which is overestimated) of decay curves for the highly exothermic reactions, and (4) the lack of a large positive activation energy for the very slow, weakly exothermic reactions. The failure of the model to be quantitative in all cases is only a failure in the sense that good fits to every acceptor cannot be obtained unless a parameter (e.g., λ_v or an alteration of ΔG° from the polar solvent value) is adjusted to account for individual characteristics of the acceptor.

This apparent success is probably forfuitous, at least in part. The solvent modes undergo fundamental changes as the medium becomes rigid. Such changes are not taken into account by the simple classical treatment of eq 4. In the future, more refined data will more severely test the adequacy of this simple approach.

F. Inhomogeneous Broadening—Distribution of Site Energies and Hopping. Guest molecules embedded in disordered media

(79) Aleksandrov, I. V.; Khairutdinov, R. F.; Zamaraev, K. I. *Dokl. Akad. Nauk SSSR* **1978**, *241*, 119. *Chem. Phys.* **1978**, *32*, 123.
(80) Strauch, S.; McLendon, G.; McGuire, M.; Guarr, T. *J. Phys. Chem.* **1983**, *87*, 3579.
(81) Foster, R. "Organic Charge Transfer Complexes"; Academic Press: London, 1969.
(82) Achiba, Y.; Kimura, K. *J. Lumin.* **1976**, *12/13*, 871.

see a range of different local solvent environments, which have been probed by lasers in "hole burning" experiments.[83] The site energy differences are reported to broaden absorption and emission spectra of the guest molecules by ≈100 cm^{-1} (≈0.01 eV). The width of the distribution of site energy differences for small, highly localized radical anions was reported to be ~0.1 eV.[84] The width for the ions used here would be expected to be smaller. From the present data we can only infer that this width is small (≤0.1 eV), using an analysis which will not be described here.

A distribution of site energies will lead to a distribution of exothermicities. Such a distribution would have no noticeable effect on decay curves for moderately exothermic reactions but would be expected to flatten the decay curves for the weakly exothermic reactions as is observed. This is, however, clearly not the principal factor shaping the decay curves because of the following: (1) A distribution of site energies would flatten decay curves for both highly exothermic reaction and weakly exothermic reactions. Instead, the highly exothermic reactions give slightly steepened decay curves. (2) The maximum of the observed rate vs. $\Delta G°$ curve shifts to higher energies and broadens with increasing time (Figures 7 and 8). A distribution of site energies would be expected to lead to a narrowing of the curve without a shift, contrary to observation. (3) The distribution of site energies would not be expected to depend strongly on temperature, while the rate of solvent relaxation would. In preliminary studies we find large temperature effects as predicted by the molecular relaxation model (see Figure S-10).

The effect of the distribution of site energies on our data would be difficult to quantitatively model and is probably small, except for very weakly exothermic reactions ($-\Delta G° < 0.2$ eV). Our neglect of it at present probably has little effect on the conclusions drawn, but there will be some uncertainty until other methods allow measurement of the width of the distribution. Linked donor–acceptor molecules held apart by a steroid spacer[42] may provide ways to measure this width. Until other methods clarify the role of site energy distributions, there will be some uncertainty about the exact relationship of ET rates to $\Delta G°$ for weakly exothermic reactions.

Although hopping to vacant donor sites (e.g., the reaction $Bip^- + Bip \rightarrow Bip + Bip^-$) has been shown to be unimportant in intermolecular ET in cryogenic glasses by experiment and by theory,[85-87] we cannot presently rule out a small effect of hopping on the very slow, weakly exothermic reactions such as biphenyl anion + naphthalene. The reason for the unimportance of hopping, even at high biphenyl concentration, is apparent from the present work: The rates of weakly exothermic ET reactions are very slow. Hopping might be greatly accelerated at higher temperatures.

G. ET Kinetics in Liquids—Energetic Information Disappears in the Diffusion Control Limit. The present results show not only that ET rates peak at intermediate exothermicities and decrease at high exothermicities but also that the failures to observe similar k vs. $\Delta G°$ plots in fluids[22-34] are an unexpected result of the diffusion control limit. The rate parameters obtained here (Table II) give the rate for donor–acceptor pairs in contact (at $R_0 = 6$ Å) as $\nu_0 F_{max} = 10^{13.6}$ s^{-1} for optimal exothermicity, $-\Delta G° = \lambda = 1.16$ eV (we shall assume that $\lambda_s \approx 0.76$ eV is appropriate for liquid MTHF). At room temperature the optimal rate is slower by a factor of ≈2 due to the $T^{-1/2}$ prefactor (eq 4), so $\nu = \nu_0 F = 10^{13.3}$ s^{-1}. This rate is ≈400 times larger than needed for the rate constant to become limited by diffusion control, i.e., for $k_d \approx k_{act}$ where $k_d = 4\pi R_0 D$ is the diffusion-limited rate constant (D is the sum of diffusion coefficients of the reactants). The rate

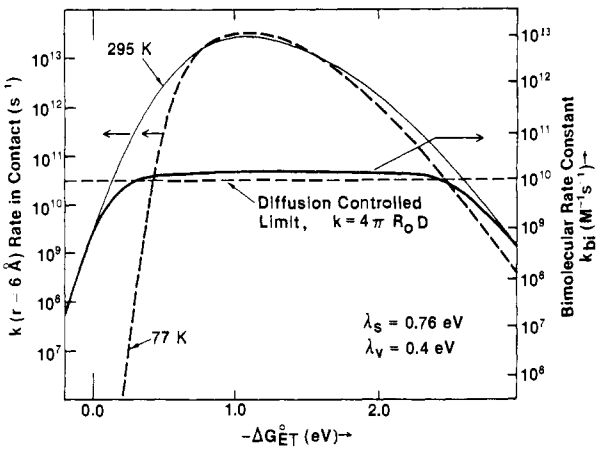

Figure 9. Use of rate vs. distance measurements in MTHF glass to predict the rate constant in fluid MTHF at room temperature: (···) $\nu = k(r = 6$ Å) at 77 K calculated with the same parameters as the line in Figure 8 and with V(6 Å) = 0.039 eV; (—) $\nu = k(r = 6$ Å) at 295 K using eq 4 to alter the dashed line for the effect of temperature. The heavy solid line is the predicted diffusional, bimolecular rate constant, k_{bi}, in MTHF at 295 K (right vertical axis). k_{bi} was calculated for $k_d = 1 \times 10^{10}$ M^{-1} s^{-1}.

constant if concentrations are not depleted near the reactants, k_{act}, is readily calculated[90,91] by integrating eq 7 over all space:

$$k_{act} = \int_0^\infty \nu \exp[-(r - R_0)/a] 4\pi r^2 g_{DA}\, dr = 4\pi\nu(aR_0^2 + 2a^2R_0 + 2a^3) \quad (15)$$

In eq 15 the reactants were treated as spheres where the distribution parameter g_{DA} was taken as 0 for $r \leq R_0$ and 1.0 for $r > R$. For $a = 0.83$ Å and $R_0 = 6$ Å, $k_{act} = 0.297\nu$ in M^{-1} s^{-1} units. Using a somewhat more complicated form[92] we find only a slight correction for adiabaticity, giving eq 16. The bimolecular rate

$$k_{act} = 0.287\nu \text{ } M^{-1} \text{ } s^{-1} \quad (16)$$

constant was calculated by using eq 16 and the well-known eq 17[93,94] for values of ν giving $k_{act} \leq k_d$. For larger ν's where k_{bi}

$$k_{bi}^{-1} = k_{act}^{-1} + k_d^{-1} \quad (17)$$

$$k_{act} \leq k_d$$

can exceed k_d due to tunneling, Pilling and Rice[95,79] solved the diffusion equation with an exponential sink term. The combination of the two calculations gives k_{bi} as a function of ν (the heavy solid line in Figure 9).

The present calculations differ only slightly from those of Marcus.[90,91] The differences are as follows: (1) We include effects of ET at greater than contact distance using the calculation of Pilling and Rice.[95,79] Thus, our maximum rate constants are a factor of ≈1.7 larger than the "diffusion control limit", which is the maximum rate constant in ref 90 and 91. (2) Effects of the adiabatic limit are included (but are small), based on $a = 0.83$ Å and $V(R_0) = 0.04$ eV from data herein. (3) Our analytic expression (eq 15) includes integration over the r^2 term also, which was possible because we assumed a simpler expression for g_{DA}. We give only the steady-state rate constant here, but note that a calculation of the transient terms should use the methods of Pilling and Rice[95,79] and should not rely on the assumptions of

(83) See, for example: Hayes, J. M.; Stout, R. P.; Small, G. J. *J. Chem. Phys.* **1980**, *73*, 4129. Friedrich, J.; Harrer, D. *Chem. Phys. Lett.* **1980**, *74*, 503. Harrer, D. *Adv. Solid State Phys.* **1980**, *20*, 341.
(84) Huddleston, R. K.; Miller, J. R. *J. Chem. Phys.* **1983**, *79*, 5337.
(85) Rice, S. A.; Kenney-Wallace, G. A. *Phys. Rev. B* **1980**, *21*, 3748.
(86) Tachiya, M. *Radiat. Phys. Chem.* **1981**, *17*, 447.
(87) Klafter, J.; Blumen, A.; Zumofen, G. *J. Phys. Chem.* **1983**, *87*, 191.
(88) Miller, J. R. *J. Phys. Chem.* **1975**, *79*, 1070.
(89) Van Leeuwen, J. W.; Heijman, M. G. J.; Nauta, H.; Casteleijn, G. *J. Chem. Phys.* **1980**, *73*, 1483.
(90) Marcus, R. A. *Int. J. Chem. Kinet.* **1981**, *13*, 865.
(91) Marcus, R. A.; Siders, P. *J. Phys. Chem.* **1982**, *86*, 622. "Mechanistic Aspects of Inorganic Reactions"; Rorabacher, D. B., Endicott, J. F., Eds.; American Chemical Society: Washington, DC, 1982; p 235.
(92) Miller, J. R., to be published.
(93) Waite, T. R. *Phys. Rev.* **1957**, *107*, 463.
(94) Marcus, R. A. *Discuss. Faraday Soc.* **1960**, *29*, 129.
(95) Pilling, M. J.; Rice, S. A. *J. Chem. Soc. Faraday Trans. 2* **1975**, *71*, 1563.

eq 17, which is not correct for $k_{act} > k_d$.

The rate constant in Figure 9 is strongly limited by diffusion and is insensitive to actual variations in ET rate from $\Delta G° \cong -0.3$ to -2.3 eV. Diffusion control, electronic excited states of products, and charge-transfer complexes were cited[38] as reasons for the failures in fluids[22-32] to observe decreasing rates at high exothermicities. The excited states and complexes are most important at very high exothermicities and are likely to nullify the decrease of k_{bi} in Figure 9. Thus, the rate vs. distance and exothermicity data from MTHF glass predict that exothermic rate restrictions will not be readily observed in solution. However, the ratio of yields of excited/ground-state products should provide a valid measure of rate constants despite the effects of diffusion control on both. This ratio is sometimes high.[36,37]

As a final note, the extrapolation to contact gave an exchange interaction $V(r = 6Å) \cong 0.04$ eV which is comparable to the 0.03-eV interaction at which ET will become adiabatic using the criterion of Brunschwig et al.[96] However, the extrapolation to 6 Å is uncertain by at least a factor of 2 so V(6 Å) is uncertain by at least a factor of $2^{1/2}$. The selection of contact distance is somewhat arbitrary. It is larger than the interplanar distance (≈4 Å) for two aromatic molecules in a sandwich configuration and smaller than the sum of the mean radii. Therefore, these calculations are not really quantitative. The debate of whether ET in fluid solutions should be described by adiabatic or non-adiabatic theories[97] would still seem, according to the present data and its uncertainties, to be a borderline call.

VI. Summary and Conclusions

Rigid glasses provide a medium in which the relation between rates and energies of intermolecular electron transfer (ET) can be measured. This provides a contrast to diffusional reactions in fluid solutions, where the true relationship of rate to energy is masked by the diffusion control limit and complexing between the colliding reactants. Furthermore, definite measurements of ET rate vs. distance are possible in glassy matrices.

In the rigid matrix used here, the ET rates decreased by orders of magnitude for reactions either too weakly or too strongly exothermic. The energy required to maximize the ET rate is larger at longer times, due primarily to greater solvation of the transient radical anion at longer times, which leads to a greater solvent reorganization for the electron-transfer processes.

At any given time, the rate vs. exothermicity relation is asymmetric: The rate climbs steeply to a maximum with increasing exothermicity but falls off less steeply beyond the maximum. The experimental rate vs. exothermicity relations are well described by a simple theory based on displaced harmonic oscillators including a group of low-frequency solvent modes which are treated classically and a group of high-frequency skeletal vibrations, represented by one mode of average frequency. The success of this theory does not guarantee its validity. The experimental rate vs. exothermicity relation may be distorted in the very weakly exothermic region ($0 < -\Delta G° < 0.2$ (eV)), if the distribution of frozen-in solvation environments has a substantial inhomogeneous width, and we cannot exclude the possibility that this distribution has a width as large as 0.1 eV. Thus, the rate vs. exothermicity relation remains somewhat uncertain in the very weakly exothermic region, which is crucial to testing the description of the low-frequency, solvent modes.

The experimental points of rate vs. exothermicity plots shows moderate scatter as expected, since changing the acceptor changes not only the exothermicity but also changes somewhat the reorganization energies of both solvent and high-frequency modes. But the very great scatter observed earlier[38,39] in the highly exothermic region for reactions of trapped electrons with the same acceptors is absent, because the present intermolecular ET reactions do not have sufficient exothermicity to produce radical ions of the acceptors in electronically excited states. The present results thus confirm the interpretation[38,39] of the trapped electron results, which focused attention on electronically excited products in highly exothermic ET reactions.

The present results are entirely consistent with recent measurements of *fixed distance* ET in fluid MTHF at room temperature,[42] which find decreasing rates at large exothermicities[42b] and reorganization energies similar to those reported here.

Registry No. Bip anion radical, 34509-93-8; 2MNap, 91-57-6; Nap, 91-20-3; Phen, 85-01-8; Tri, 217-59-4; M_2Ql, 877-43-0; Bpln, 259-79-0; BzQl, 230-27-3; Ph_3Et, 58-72-0; Pyr, 129-00-0; Flth, 206-44-0; Acnp, 208-96-8; Acd, 260-94-6; Cnal, 104-55-2; Bcin, 230-17-1; AzBz, 103-33-3; NBz, 98-95-3; Phenz, 92-82-0; Fln, 486-25-9; MA, 108-31-6; MQ, 553-97-9; MNQ, 58-27-5; tB_2Q, 2460-77-7; BQ, 106-51-4; DNBz, 100-25-4; Cl_2Q, 615-93-0; F_4Q, 527-21-9; Cl_4Q, 118-75-2; TCNE, 670-54-2.

Supplementary Material Available: Reaction rate curves of the biphenyl anion (12 pages). Ordering information is given on any current masthead page.

(96) Brunschwig, B. S.; Logan, J.; Newton, M. D.; Sutin, N. *J. Am. Chem. Soc.* **1980**, *102*, 5798.

(97) See comments in ref 15, pp 96–105, 295–299.